Inpainting via sub-Riemannian minimizers on the group of rototranslations*

Andrei A. Ardentov and Yuri L. Sachkov

Program Systems Institute, Pereslavl-Zalessky, Russia,
E-mail: aaa@pereslavl.ru, sachkov@sys.botik.ru

Abstract. The paper describes an approach to monochrome image inpainting by completing damaged isophotes (level lines of brightness) by optimal curves for the left-invariant sub-Riemannian problem on the group of rototranslations (motions) of a plane SE(2). The approach and the algorithm for computation of completing isophotes are presented in detail.

Keywords: Image inpainting, sub-Riemannian geometry, neurogeometry of vision, group of rototranslations of a plane

1 Image inpainting, neurogeometry of vision and sub-Riemannian geometry

The task of restoring damaged or latent images is one of actual problems in computer graphics, photo restoration, film and painting. A number of methods were suggested to solve this problem, many of which are based on advanced mathematical techniques, in particular, on the application of the calculus of variations and optimal control [2–5].

This paper is based on provisions a new direction of neuroscience — neurogeometry [6,7], as well as on recent results of sub-Riemannian geometry [8–10]. On the basis of results of these studies were developed an algorithm and a parallel software to restore monochrome binary or halftone images represented as series of isophotes (level lines of brightness).

1.1 Neurogeometry of vision

An important recent discovery of neurophysiology is a geometric structure corresponding to the primary visual cortex of the human brain. The primary visual cortex performs a primary (preceding any treatment) perception of visual information by the human brain. It was established [6,7] that in order to save images, the primary cortex simulates the contact structure $\{(x, y, p)\} = D \times \mathbb{R}P^1$ on the

* Supported by Russian Foundation for Basic Research, Project No. 09-01-00246-a, and by The SKIF Supercomputer Project of the Russia-Belarus Union State [1]

surface of the retina $D \subset \mathbb{R}^2$. Here, the tangent element p is the slope of the curve $y(x)$ at the point x. It turned out that for effective imaging, for the human brain it is profitable to keep a contour not as a set of successive points (x_i, y_i), but as a set of strokes (x_i, y_i, p_i), in the limit — in the form of a continuous curve $(x(t), y(t), p(t))$, $p = dy/dx$. If part of the curve is damaged or hidden from observation, the missing arc is restored on the basis of the following variational principle: the restored arc should have minimum Euclidean length in the space of contact elements (x, y, θ), $\theta = \arctan p$:

$$\int \sqrt{\dot{x}^2 + \dot{y}^2 + \dot{\theta}^2}\, dt \to \min. \tag{1}$$

(If the Euclidean length would be computed in the plane (x, y), then the arc would be trivially and erroneously restored by a straight line segment). The variational principle (1) is taken in this work as a basis of the method of restoring a hidden arc. The described internal geometry of the visual cortex is one of the main objects of study of neurogeometry of vision — a direction of neurophysiology which studies the geometric structure of the human brain simulating the spatial images of the external world.

1.2 Statement of the problem of image reconstruction and method of solution

We consider the problem of recovering a monochrome (binary of gray-scale) image, some fragments of which are corrupted or hidden from observation. The goal is to restore the damaged parts of the image in an anthropomorphic (natural for a human being) way. Mathematically, the problem can be formalized as follows. Given a domain $D \subset \mathbb{R}^2$, mutually disjoint subdomains

$$O_1, ..., O_N \subset D, \tag{2}$$

and a function $f : D \setminus (\bigcup_{i=1}^{N} O_i) \to [0, 1]$, one should restore the function f in the domains $O_1, \ldots, O_N$. Here D is the domain of the initial image, O_i are subdomains with corrupted image, and the function f determines the image (brightness for gray-scale image, and for binary image it is a function, whose level lines coincide with the curves constituting the image). We propose to restore the image in subdomains O_i by completing isophotes — level curves of f in these subdomains (in the case of halftone images, the strips between the reconstructed curves are painted according to the brightness values on these curves). The reconstructing curves are calculated via the variational approach (1): the constructed curve $(x(t), y(t))$ should minimize the distance in the space (x, y, θ), where (x, y) are coordinates in the plane $\mathbb{R}^2$ and $\theta(t) = \arctan p(t) = \arctan(\dot{y}/\dot{x})$ is the slope of the tangent to the curve $(x(t), y(t))$. In this work we describe an algorithm for solving the corresponding optimal control problem on the basis of papers [8–10]. In the further work [21] is described the corresponding set of parallel software for reconstruction of corrupted images.

Our approach seems successful under the following assumptions:

– Isophotes of an image can be represented by level lines of a smooth function $f : D \to [0,1]$,
– The function f has no critical points in the corrupted subdomains $O_1, \ldots, O_N \subset D$,
– Information on intersection points of level lines of f with boundaries of O_i can be effectively extracted from the image.

We believe that under these assumptions the proposed method can be successfully used in combination with other methods of image inpainting.

2 Reconstruction of isophotes via variational approach

Consider a smooth flat curve $AB = \{(x(t), y(t)) \mid t \in [a,b]\}$. Suppose that a part of this curve $CD = \{(x(t), y(t)) \mid t \in [c,d]\}$ is hidden from observation or damaged. To restore the curve CD, construct the tangent T_C to the curve AC at the point C and the tangent T_D at the point D, see Fig. 1. Denote by θ_c, θ_d the slope of the tangents T_C, T_D. The required curve $\overline{CD} = \{(\overline{x}(t), \overline{y}(t)) \mid t \in [c,d]\}$ should start at the point C with the slope θ_c, terminate at the point D with the slope θ_d, and have the minimum Euclidean length in the space (x, y, θ), see (1). The boundary conditions imply a smooth conjugation of the restored curve $\overline{CD}$ with the known arcs AC and DB of the original curve. The original and restored curves are shown in Fig. 2. The minimum condition (1) formalizes a natural condition for the new curve $\overline{CD}$: in its search, large deviations are penalized both in the coordinates (x, y), and in the angle θ. Thus, there is minimized a certain integral compromise between the linear and angular velocities of the curve. Moreover, one can minimize a more general length functional reflecting the different weights of space variables (x, y) and the angle variable θ:

$$\int \sqrt{\dot{x}^2 + \dot{y}^2 + \alpha^2 \dot{\theta}^2}\, dt \to \min, \qquad \alpha > 0, \tag{3}$$

this extension is easily performed by the change of variables

$$x = \alpha\widetilde{x}, \quad y = \alpha\widetilde{y}, \quad \theta = \widetilde{\theta}, \quad u_1 = \alpha\widetilde{u}_1, \quad u_2 = \widetilde{u}_2. \tag{4}$$

Examples of curves restored via the approach described are presented in Figs. 3, 4.

3 Sub-Riemannian geometry on the group of motions of a plane

Problem (1) is formalized as the following optimal control problem [14]:

$$\dot{x} = u_1 \cos\theta, \quad \dot{y} = u_1 \sin\theta, \quad \dot{\theta} = u_2, \tag{5}$$

$$q = (x, y, \theta) \in M = \mathbb{R}^2_{x,y} \times S^1_\theta, \quad u = (u_1, u_2) \in \mathbb{R}^2, \tag{6}$$

$$q(0) = q_0 = (0,0,0), \qquad q(t_1) = q_1 = (x_1, y_1, \theta_1), \tag{7}$$

$$l = \int_0^{t_1} \sqrt{u_1^2 + u_2^2}\, dt \to \min. \tag{8}$$

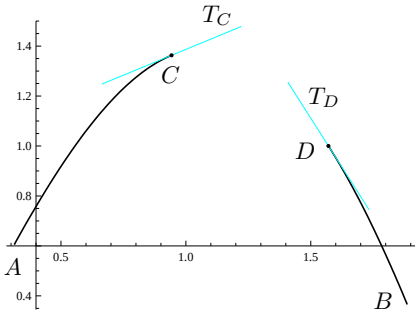

Fig. 1. Boundary conditions for restoration of the arc CD

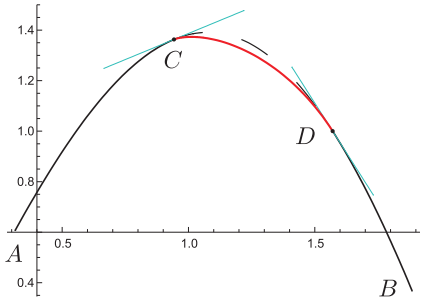

Fig. 2. Curve AB with original and restored arcs CD

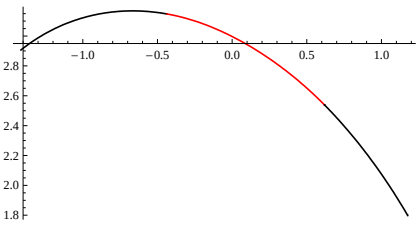

Fig. 3. Restored convex isophote

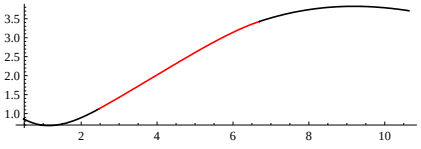

Fig. 4. Restored isophote with inflection point

The state space of this problem $M = \mathbb{R}^2_{x,y} \times S^1_\theta$ is naturally identified with the group SE(2) of orientation-preserving motions (rototranslations) of a two-dimensional plane, which is represented by 3×3 matrices as follows:

$$\mathrm{SE}(2) = \left\{ \begin{pmatrix} \cos\theta & -\sin\theta & x \\ \sin\theta & \cos\theta & y \\ 0 & 0 & 1 \end{pmatrix} \mid \theta \in S^1 = \mathbb{R}/(2\pi\mathbb{Z}),\ x, y \in \mathbb{R} \right\}.$$

Then problem (5)–(8) is obviously reformulated as a left-invariant sub-Riemannian problem on the Lie group SE(2) [14, 15]. Consider a rank 2 nonintegrable left-invariant sub-Riemannian structure on SE(2), i.e., a rank 2 nonintegrable left-invariant distribution Δ on SE(2) with a left-invariant inner product $\langle \cdot, \cdot \rangle$ on Δ. One can easily show that such a structure is unique, up to a constant scalar factor in the inner product. We choose the following model for such a sub-Riemannian structure:

$$\begin{aligned} &\Delta_q = \mathrm{span}(X_1(q), X_2(q)), \qquad \langle X_i, X_j \rangle = \delta_{ij}, \quad i,\ j = 1, 2, \\ &X_1(q) = qE_{13}, \quad X_2(q) = q(E_{21} - E_{12}), \qquad q \in \mathrm{SE}(2), \end{aligned}$$

(where E_{ij} denotes the 3×3 matrix with identity entry in row i and column j, and zero entries elsewhere) and study the corresponding optimal control problem:

$$\begin{aligned} &\dot{q} = u_1 X_1(q) + u_2 X_2(q), \qquad q \in M = \mathrm{SE}(2), \quad u = (u_1, u_2) \in \mathbb{R}^2, \\ &q(0) = q_0 = \mathrm{Id}, \qquad q(t_1) = q_1, \\ &l = \int_0^{t_1} \sqrt{u_1^2 + u_2^2}\, dt \to \min. \end{aligned}$$

The problem can be reformulated in robotics terms as follows. Consider a mobile robot in the plane that can move forward and backward, and rotate around itself (Reeds-Shepp car) [16]. The state of the robot is described by coordinates (x, y) of its center of mass and by angle of orientation θ. Given an initial and a terminal state of the car, one should find the shortest path from the initial state to the terminal one, when the length of the path is measured in the space (x, y, θ), see Fig. 5.

Problem (5)–(8) is important for diffusion equation on SE(2) [17–20].

It was shown in work [8] that problem (5)–(8) has an optimal solution for any terminal point $q_1 \in \mathrm{SE}(2)$.

3.1 Reduction of problem (5)–(8) to solving systems of equations

In this subsection we describe some results of papers [8–10] that allow us to reduce problem (5)–(8) to solving systems of equations in elliptic functions.

Via Pontryagin Maximum Principle [11, 14], extremal trajectories in problem (5)–(8) are parameterized by points of the phase cylinder $C = (2S^1_\gamma) \times \mathbb{R}_c$ of the pendulum

$$\dot{\gamma} = c, \qquad \dot{c} = -\sin\gamma. \tag{9}$$

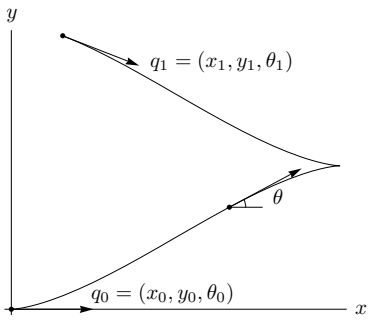

Fig. 5. Statement of problem (5)–(8)

The family of arc-length parametrized extremal trajectories in problem (5)–(8) is described by the exponential mapping

$$\begin{aligned}&\mathrm{Exp} : N \to M, \qquad N = C \times \mathbb{R}_+,\\ &\mathrm{Exp}(\nu) = \mathrm{Exp}(\lambda, t) = q(t), \qquad \nu = (\lambda, t) = (\gamma, c, t) \in N.\end{aligned}$$

The equation of pendulum (9) has the energy integral $E = \dfrac{c^2}{2} - \cos\gamma \in [-1, +\infty)$. Consider the following decomposition of the cylinder C into disjoint invariant sets of the pendulum:

$$\begin{aligned}&C = \bigcup_{i=1}^{5} C_i, \qquad (10)\\ &C_1 = \{\lambda \in C \mid E \in (-1, 1)\},\\ &C_2 = \{\lambda \in C \mid E \in (1, +\infty)\},\\ &C_3 = \{\lambda \in C \mid E = 1,\ c \neq 0\},\\ &C_4 = \{\lambda \in C \mid E = -1\} = \{(\gamma, c) \in C \mid \gamma = 2\pi n,\ c = 0\}, \quad n \in \mathbb{N},\\ &C_5 = \{\lambda \in C \mid E = 1,\ c = 0\} = \{(\gamma, c) \in C \mid \gamma = \pi + 2\pi n,\ c = 0\}.\end{aligned}$$

In work [8] were introduced elliptic coordinates (φ, k) on the domain $C_1 \cup C_2 \cup C_3$ of the cylinder C, where k is a reparametrized energy, and φ is the time of motion of the pendulum (9). In the elliptic coordinates the flow of the pendulum (9) rectifies: $\dot\varphi = 1$, $\dot k = 0$. Using these coordinates we obtained the following parametrization of extremal trajectories.

If $\lambda = (\varphi, k) \in C_1$, then $\varphi_t = \varphi + t$ and:

$$\begin{aligned}&\cos\theta_t = \mathrm{cn}\,\varphi\,\mathrm{cn}\,\varphi_t + \mathrm{sn}\,\varphi\,\mathrm{sn}\,\varphi_t,\\ &\sin\theta_t = s_1(\mathrm{sn}\,\varphi\,\mathrm{cn}\,\varphi_t - \mathrm{cn}\,\varphi\,\mathrm{sn}\,\varphi_t),\\ &\theta_t = s_1(\mathrm{am}\,\varphi - \mathrm{am}\,\varphi_t) \pmod{2\pi},\\ &x_t = (s_1/k)[\mathrm{cn}\,\varphi(\mathrm{dn}\,\varphi - \mathrm{dn}\,\varphi_t) + \mathrm{sn}\,\varphi(t + \mathrm{E}(\varphi) - \mathrm{E}(\varphi_t))],\\ &y_t = (1/k)[\mathrm{sn}\,\varphi(\mathrm{dn}\,\varphi - \mathrm{dn}\,\varphi_t) - \mathrm{cn}\,\varphi(t + \mathrm{E}(\varphi) - \mathrm{E}(\varphi_t))].\end{aligned}$$

In the domain C_2, it will be convenient to use the coordinate $\psi = \varphi/k$, $\psi_t = \varphi_t/k = \psi + t/k$. If $\lambda \in C_2$, then:

$$\begin{aligned}
&\cos\theta_t = k^2 \operatorname{sn}\psi \operatorname{sn}\psi_t + \operatorname{dn}\psi \operatorname{dn}\psi_t,\\
&\sin\theta_t = k(\operatorname{sn}\psi \operatorname{dn}\psi_t - \operatorname{dn}\psi \operatorname{sn}\psi_t),\\
&x_t = s_2 k[\operatorname{dn}\psi(\operatorname{cn}\psi - \operatorname{cn}\psi_t) + \operatorname{sn}\psi(t/k + \mathrm{E}(\psi) - \mathrm{E}(\psi_t))],\\
&y_t = s_2[k^2 \operatorname{sn}\psi(\operatorname{cn}\psi - \operatorname{cn}\psi_t) - \operatorname{dn}\psi(t/k + \mathrm{E}(\psi) - \mathrm{E}(\psi_t))].
\end{aligned}$$

Here and below we use Jacobi's functions $\operatorname{am}(\varphi,k)$, $\operatorname{cn}(\varphi,k)$, $\operatorname{sn}(\varphi,k)$, $\operatorname{dn}(\varphi,k)$, $\mathrm{E}(\varphi,k)$; moreover, $K(k)$ is the complete elliptic integral of the first kind [13]. If $\lambda \in \cup_{i=3}^{5} C_1$, then extremal trajectories are parameterized by elementary functions [8].

Consider the following decomposition of $M = \mathrm{SE}(2) = \mathbb{R}^2_{x,y} \times S^1_\theta$ depending on values of the functions $R_1 = y\cos\frac{\theta}{2} - x\sin\frac{\theta}{2}$, $R_2 = x\cos\frac{\theta}{2} + y\sin\frac{\theta}{2}$:

$$\begin{aligned}
&\widetilde{M} = \{q \in M \mid R_1(q)R_2(q)\sin\theta \neq 0\},\\
&\widetilde{M} = \cup_{i=1}^{8} M_i, \qquad M_i \cap M_j = \emptyset \ \forall\, i \neq j,\\
&M' = \{q \in M \mid R_1(q)R_2(q)\sin\theta = 0\},
\end{aligned}$$

where each of the sets M_i is determined by constant signs of the functions $\sin\theta$, R_1, R_2 described in Table 1.

M_i	M_1	M_2	M_3	M_4	M_5	M_6	M_7	M_8
$\operatorname{sgn}(\sin\theta)$	$-$	$-$	$-$	$-$	$+$	$+$	$+$	$+$
$\operatorname{sgn}(R_1)$	$+$	$+$	$-$	$-$	$-$	$-$	$+$	$+$
$\operatorname{sgn}(R_2)$	$+$	$-$	$-$	$+$	$+$	$-$	$-$	$+$

Table 1. Definition of domains M_i

Preimage of the exponential mapping is the Cartesian product $N = C \times \mathbb{R}_+$. In [9,10] was obtained a global description of the cut time

$$t_{\mathrm{cut}}(\lambda) = \sup\{t_1 > 0 \mid q_s \text{ is optimal for } s \in [0,t_1]\}, \qquad \lambda \in C,$$

along extremal trajectories of problem (5)–(8). In work [10] were defined the sets

$$\widehat{M} = M \setminus \{q_0\}, \qquad \widehat{N} = \{(\lambda,t) \in N \mid t \leq t_{\mathrm{cut}}(\lambda)\}.$$

Since for any $q_1 \in M$ an optimal control exists, then the mapping $\mathrm{Exp} : \widehat{N} \to \widehat{M}$ is surjective; although, it has multiple (Maxwell) points, thus it is not injective. Further, in works [9, 10] were defined an open dense subset $\widetilde{N} \subset \widehat{N}$, and its decomposition into disjoint subsets $\widetilde{N} = \cup_{i=1}^{8} D_i$, such that the exponential mapping has the following global structure:

$$\mathrm{Exp} : \widetilde{N} \to \widetilde{M} \text{ and all } \mathrm{Exp} : D_i \to M_i \text{ are diffeomorphisms.} \qquad (11)$$

4 Algorithm for image inpainting

This section describes the algorithm `GlobalSolve` of restoring images via the variational principle (3) on the basis of results described in the previous section. The general structure of the algorithm is presented in Fig. 6. From the top to the bottom, `GlobalSolve` consists of the following subalgorithms:

- `RestoreDomain` restores corrupted isophotes in a subdomain O_k, $k = 1, \ldots, N$ (2), see Subsec. 4.4,
- `FindRoot` numerically evaluates parameters that determine a corrupted isophote $(x(t), y(t))$ from its boundary conditions $q_1 = (x_1, y_1, \theta_1)$ (7), see Subsec. 4.2,
- `Solver` solves a system of 3 algebraic equations in 3 elliptic functions

$$\mathrm{Exp}(\nu) = q_1, \qquad q_1 \in M_i, \quad \nu \in D_i \tag{12}$$

  for its root $\nu \in D_i \cap C_j$, $j \in \{1, 2\}$, see Subsec. 4.1,
- `RemoveCusp` aims to remove cusps at optimal trajectories $(x(t), y(t))$ by appropriate change of the parameter α (3), see Subsec. 4.3.

The algorithm `GlobalSolve` was realized by a parallel software `OptimalInpainting` described in [21].

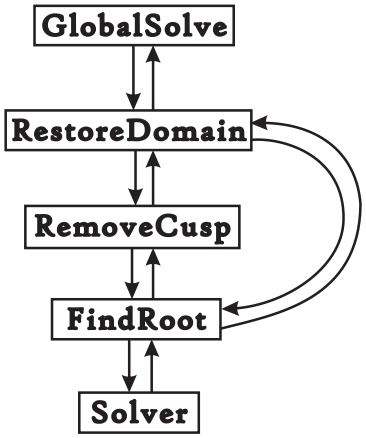

Fig. 6. General structure of the algorithm

4.1 Algorithm `Solver` for solving system of equations (12)

`Input:` $q_1 \in M_i$, `initial` $\in \{$`true`, `false`$\}$, $j \in \{1, 2\}$, $i \in \{1, \ldots, 4\}$, $\nu \in D_i \cap C_j$.

`Output:` $\nu \in D_i \cap C_j$.
`Performed actions:` The algorithm searches numerically for an approximate root $\nu \in D_i \cap C_j$ of system (12) with a prescribed accuracy ε. The variable ν is both an input parameter (initial approximation of the root in the case `initial` = `true`) and an output parameter (the root found).
`Constants of the algorithm:` `maxiteration`, `maxiterrnd` $\in \mathbb{N}$, $\varepsilon > 0$.

`Steps of the algorithm:`

1. If `initial` = `true`, then go to step 3.
2. Initial approximation ν is selected randomly in the subdomain $D_i \cap C_j$.
3. An iterative algorithm of search for an approximate root of system (12) is started from the initial point ν. If the number of iterations of this algorithm exceeds `maxiteration`, then go to step 2. If $\nu \notin D_i \cap C_j$, then go to step 2. If the total number of iterations of the algorithm `Solver` exceeds `maxiterrnd`, then the algorithm terminates (the root was not found).
4. If $|\operatorname{Exp}(\nu) - q_1| < \varepsilon$, then the algorithm terminates and returns the value of the root ν.

4.2 Algorithm `FindRoot` for computing an optimal trajectory of problem (5)–(8)

`Input:` $q_1 \in M$, `initial` $\in \{$`true`, `false`$\}$, $j \in \{1, 2\}$, $\nu \in C_j$.
`Output:` $j \in \{1, 2\}$, $\nu \in C_j$.
`Performed actions:` The algorithm finds numerically a root ν of system (12) and the number j of the domain C_j such that $\nu \in C_j$. The parameter α (4) is set equal to 1. The variables ν and j are both input parameters (initial approximation of the root and the number of the domain which contains this root in the case `initial` = `true`) and output parameters (the root found).

`Steps of the algorithm:`

1. The number i of the domain M_i such that $q_1 \in M_i$ is computed by Table 1.
2. If `initial` = `true`, then go to step $(j + 2)$, i. e., 3 or 4.
3. The algorithm `Solver` is run with the parameters q_1, `initial`, i, $j = 1$, ν. If the root is found, then the algorithm terminates successfully, otherwise `initial` := `false`.
4. The algorithm `Solver` is run with the parameters q_1, `initial`, i, $j = 2$, ν. If the root is found, then the algorithm terminates successfully, otherwise `initial` := `false` and go to step 3.

Given a root $\nu = (\lambda, t_1)$ of system (12), the corresponding optimal trajectory of problem (5)–(8) is $q(t) = \operatorname{Exp}(\lambda, t)$, $t \in [0, t_1]$. Although, optimal trajectories of problem (5)–(8) may have cusps (see Fig. 5), which seems not appropriate for isophotes of images being reconstructed. One can often remove cusps by changing the parameter α (4), see Subsec. 4.3.

4.3 Algorithm `RemoveCusp` for removal of cusps on isophotes

`Input:` $q_1 = (x_1, y_1, \theta_1) \in M$.
`Output:` $\alpha > 0$, $j \in \{1, 2\}$, $\nu \in C_j$.
`Performed actions:` The algorithm searches for a value of $\alpha > 0$ such that the optimal trajectory $(x(t), y(t))$ of the problem (5)–(7) with the cost functional

$$l_\alpha = \int_0^{t_1} \sqrt{u_1^2 + \alpha^2 u_2^2}\, dt \to \min \tag{13}$$

has no cusps. The new problem (5)–(7), (13) is reduced to the original problem (5)–(8) by the change of coordinates (4).
`Constants of the algorithm:` $\Delta\alpha = 0.1$,

$$\alpha_{\texttt{init}} = 0.6\frac{\pi - |\theta_1 - \pi| + 0.7\frac{|y_1|}{|x_1+0.2|}}{0.05 + \sqrt{x_1^2 + y_1^2}} + 0.2.$$

`Steps of the algorithm:`

1. Initial values of $\alpha := \alpha_{\texttt{init}}$, `initial` := `false` are set.
2. $(x_\alpha, y_\alpha) := (\alpha x_1, \alpha y_1)$.
3. The algorithm `FindRoot` is run with the parameters $(x_\alpha, y_\alpha, \theta_1)$, `initial`, j, ν.
4. If the root ν computed by `FindRoot` corresponds to a curve $(x(t), y(t))$ without cusps (i.e., $\dot{x}^2(t) + \dot{y}^2(t) \neq 0$), then the algorithm terminates successfully.
5. `initial` := `true`, $\alpha := \alpha + \Delta\alpha$ and go to step 2.

Examples of recovered images with and without cusps are given in Figs. 7 and 8. These images were obtained respectively without and with change of the parameter α.

The diffeomorphic property (11) of the mapping Exp is used in this algorithm: close points in the preimage of the exponential mapping are transformed by Exp to close points in its image. The same property (11) is used below in the algorithm `RestoreDomain`, see Subsec. 4.4.

4.4 Algorithm `RestoreDomain` for computing isophotes in a corrupted domain

`Input:` $k \in \mathbb{N}$.
`Output:` text file `outputs<k>`.
`Performed actions:` The number k corresponds to the input file `inputs<k>` which contains coordinates of endpoints q_1 of all isophotes for the corrupted domain $O_k \subset D$ (2). The algorithm finds all the parameters for restoring these isophotes and writes them to the file `outputs<k>`.

`Steps of the algorithm:`

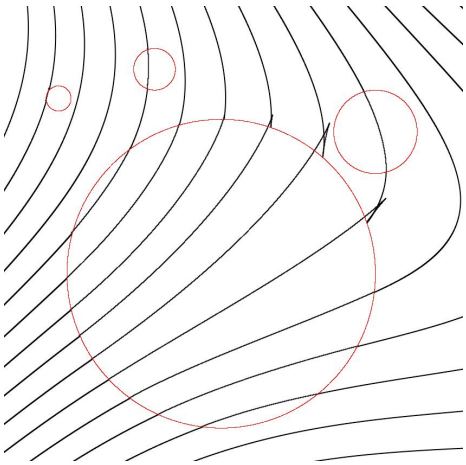

Fig. 7. Recovered image with cusps

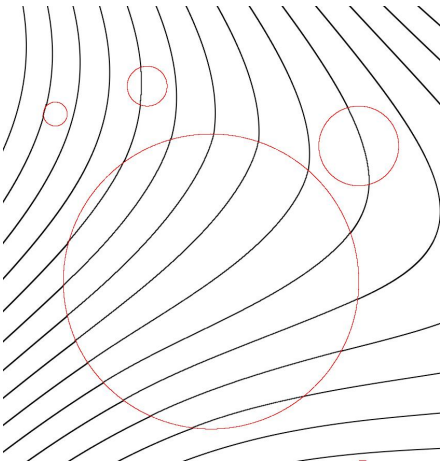

Fig. 8. Recovered image without cusps

1. `initial` := `false`.
2. The input data $q_1 = (x_1, y_1, \theta_1)$ for the current isophote is read from the file `inputs<k>`. If the file is empty, then the algorithm terminates.
3. If `initial` = `true`, then $\alpha_0 := \alpha + \texttt{sign}(\alpha - \alpha_{\texttt{init}})\Delta\alpha$ and the algorithm `FindRoot` is run with the parameters $(\alpha_0 x_1, \alpha_0 y_1, \theta_1)$, `initial`, ν, j. If the root ν computed by `FindRoot` corresponds to a curve without cusps, then the required root is found, go to step 5. Otherwise $\alpha_0 := \alpha_{\texttt{init}} + \texttt{sign}(\alpha_{\texttt{init}} - \alpha)\Delta\alpha$ and the algorithm `FindRoot` is run with the parameters $(\alpha_0 x_1, \alpha_0 y_1, \theta_1)$, `initial`, ν, j. If the root ν computed by `FindRoot` corresponds to a curve without cusps, then the required root is found, go to step 5.
4. The algorithm `RemoveCusp` is run with the input q_1.
5. The parameters α, ν, j are written to the file `outputs<k>`, go to step 2.

Since the calculation of the parameters for the trajectories from different corrupted domains occurs independently, then it makes sense to evaluate them in parallel. This was realized in a parallel software for image inpainting [21].

This paper describes in detail an approach to monochrome image inpainting via completing damaged isophotes by sub-Riemannian length minimizers for the left-invariant sub-Riemannian problem on the group of motions of a plane SE(2). The approach and the algorithm presented in this work were realized by a set of parallel software `OptimalInpaiting` presented in a further work [21].

The authors thank A.P.Mashtakov for participation in the work on this paper.

References

1. The SKIF Supercomputer Project of the Russia-Belarus Union State, http://skif-grid.botik.ru/

2. Chan T.F., Kang S.H., Shen J.: Euler's elastica and curvature based inpainting. SIAM Journal of Applied Math. 63, 564–592 (2002)
3. Citti G., Sarti A.: A cortical based model of perceptual completion in the roto-translation space, J. Math. Imaging Vis. 24: 307–326, 2006.
4. Esedoglu S., Shen J., Digital image inpainting by the Mumford-Shah-Euler image model, Europ. J. Appl. Math., 13 : 353-370, 2002.
5. Kimia B.B., Frankel I., Popescu A.-M., Euler spiral for shape completion, Int. J. Comp. Vision, 54 :159-182, 2003.
6. Petitot J.: The neurogeometry of pinwheels as a sub-Riemannian contact structure, J. Physiology - Paris, 97 (2003), 265–309.
7. Petitot J.: Neurogeometrie de la vision — Modeles mathematiques et physiques des architectures fonctionnelles, Editions de l'Ecole Polytechnique (2008)
8. Moiseev I., Sachkov Yu. L.: Maxwell strata in sub-Riemannian problem on the group of motions of a plane, ESAIM: COCV, *ESAIM: COCV*, 16 (2010), 380–399, available at arXiv:0807.4731v1, 29 July 2008.
9. Sachkov Yu. L.: Conjugate and cut time in the sub-Riemannian problem on the group of motions of a plane, ESAIM: COCV, 16 (2010), 1018–1039.
10. Sachkov Yu. L.: Cut locus and optimal synthesis in the sub-Riemannian problem on the group of motions of a plane, ESAIM: COCV, 2011 (accepted).
11. Pontryagin L.S., Boltyanskii V.G., Gamkrelidze R.V., Mishchenko E.F.: The mathematical theory of optimal processes, Wiley Interscience, 1962.
12. Ardentov A.A., Sachkov Yu. L.: Solution of Euler's elastic problem (in Russian), Avtomatika i Telemekhanika, 2009, No. 4, 78–88. (English translation in Automation and remote control.)
13. Whittaker E.T., Watson G.N.: A Course of Modern Analysis. An introduction to the general theory of infinite processes and of analytic functions; with an account of principal transcendental functions, Cambridge University Press, Cambridge (1996)
14. Agrachev A.A., Sachkov Yu. L.: Control Theory from the Geometric Viewpoint, Springer-Verlag, Berlin 2004.
15. Montgomery R.: A Tour of Subriemannian Geometries, Their Geodesics and Applications. American Mathematical Society (2002).
16. Laumond J.P.: Nonholonomic motion planning for mobile robots, Lecture notes in Control and Information Sciences, 229. Springer (1998).
17. Duits R., van Almsick M.: The Explicit Solutions of Linear Left-Invariant Second Order Stochastic Evolution Equations on the 2D Euclidean Motion Group. Quarterly of Applied Mathematics, Volume 66, no. 1, pp. 27-67, April 2008.
18. Duits R., Franken,E.M.: Left-invariant parabolic Evolutions on SE(2) and Contour Enhancement via Invertible Orientation Scores. Part II: Nonlinear Left-invariant Diffusions on invertible Orientation Scores. Quarterly of Applied Mathematics, Volume 68, no. 2, pp. 293-331, June 2008.
19. Duits R., Franken,E.M.: Left-invariant parabolic Evolutions on SE(2) and Contour Enhancement via Invertible Orientation Scores. Part I: Linear Left-invariant Diffusion Equations on SE(2). Quarterly of Applied Mathematics, Volume 68, no. 2, pp. 255-292, June 2008.
20. Agrachev A.A., Boscain U., Gauthier J.P., Rossi F., The intrinsic hypoelliptic Laplacian and its heat kernel on unimodular Lie groups, Journal of Functional Analysis. Vol. 256 (2009). No. 8, pp. 2621–2655.
21. Mashtakov A.P., Sachkov Yu.L.: `OptimalInpaiting` parallel software for image inpainting via sub-Riemannian minimizers, submitted.